



## AN ABSTRACT OF THE THESIS OF

Hidekel A. Moreno Luna for the degree of Honors Bachelor of Science in Advanced Chemistry on October 14, 2011.

Title: Thin-Film Dielectric Structure of Spin-Coated ZrO<sub>2</sub> from Aqueous Inorganic Solution

Abstract approved:

---

Douglas A. Keszler

An inorganic aqueous precursor for the deposition of ZrO<sub>2</sub> thin films via spin-coating was developed. Hydrolysis and condensation chemistries of ZrOCl<sub>2</sub>·8H<sub>2</sub>O were used as the principal reactions to guide the synthesis. Refractive index,  $n$ , for a film annealed at 300 °C at 550 nm was measured to be  $n=1.97$  by SE. Thin-films remained amorphous until about 500 °C with slight signs of monoclinic phase at 400 °C, as determined by XRD. FT-IR analysis of thin films showed remaining hydration until 400 °C annealing temperatures. A second order mathematical model was also developed for the metal oxide thickness as a function of precursor concentration with a minimum experimental thickness for this deposition system of 1.02(8) nm.

Key words: pin-coating, environmentally friendly electronics, inorganic chemistry of ZrO<sub>2</sub>, ZrO<sub>2</sub> thin-film deposition

Corresponding e-mail address: [morenoh@onid.orst.edu](mailto:morenoh@onid.orst.edu)

©Copyright by Hidekel A. Moreno Luna  
October 14, 2011  
All Rights Reserved

Thin-Film Dielectric Structure and Performance of Spin-Coated ZrO<sub>2</sub> from  
Aqueous Inorganic Solution

by  
Hidekel A. Moreno Luna

A THESIS

submitted to

Oregon State University

University Honors College

in partial fulfillment of the requirements of the degree of  
Honors Baccalaureate of Science in Advanced Chemistry (Honors Associate)

Presented October 14, 2011  
Commencement June 2012

Honors Baccalaureate of Science in Advanced Chemistry thesis of Hidekel A. Moreno Luna presented on October 14, 2011.

APPROVED:

---

Major Professor, representing Materials Science

---

Committee Member, representing Inorganic Chemistry

---

Committee Member, representing Materials Science

---

Chair, Department of Chemistry

---

Dean, University Honors College

I understand that my thesis will become part of the permanent collection of Oregon State University, Honors College. My signature below authorizes release of my thesis to any reader upon request.

---

Hidekel A. Moreno Luna, Author

## ACKNOWLEDGEMENTS

Through my undergraduate academic studies there have been a number of people that have fostered my chemistry curiosity where their ideas and theories have been imprinted for life. I would first like to thank Dr. Keszler who gave me the opportunity to learn a little of the art of deposition from aqueous precursors and for the attention that has brought my success. A group of graduate students has also given valuable insights in major steps of this project. I would like to thank to Sharon Betterton for her guidance and her friendship. Emmeline for teaching me ellipsometry and X-Ray reflectivity, Robert for his knowledge in XRD, Wei for his help in electronics making, Kris for his optimism in needed times, and everyone else in the group who helped in one way or another.

Several wonderful teachers have taught me both the practice and theory of chemistry from organic to inorganic chemistry: Drs. Pastorek, Lerner, Firpo, Loeser, Chong, Evans, Kong, and Maier. Very warm thanks is given to Dr. Nibler for his advising over the last few years and for being always willing to talk about future academic decisions. Likewise, Rebekah Lancelin for her advising. For all the chemistry staff, especially Kristi Edwards. Also for the friendship of chemistry students through many hours of data workup and writing, including: Jamie, Brad, Darren, Michael, Corey, Lyle, many of whom I am privileged to call *amigos* (Spanish-friends).

For monetary funds I would like to thank the NSF and Center for Green Materials Chemistry. I would also like to thank the support from my family, my mother, my father, my brother, and for the company of my sister in many of my life adventures. And finally to all members of the committee: Dr. Douglas Keszler, Dr. Michael Lerner, and Wei Wang for the time and help they brought to this project.

## CONTRIBUTION OF AUTHORS

Sharon Betterton in Chapter 2 for her consultation during the writing..

Christine Pastorek who assisted with IR collection in Chapter 2. Emmeline

Altschul who helped with initial ellipsometry work in Chapter 2. Robert

Kikineshi for his assistance in XRD collection in Chapter 2. Wei Wang for

assistance in MIM capacitor making and testing Chapter 2. Dr. Keszler for

providing insights in both theoretical and practical for this thesis.



# TABLE OF CONTENTS

<u>Figure</u>	<u>Page</u>
1. Introduction.....	1
1.1. Current status of high-k dielectrics.....	2
1.2. Group IVB metal oxide thin-films.....	4
1.3. Thin-film deposition methods .....	5
1.4. Summary.....	10
References.....	11
2. Aqueous Solution Chemistries and Electric Characteristics for Solution Deposited Zirconium (IV) Oxide.....	12
2.1. Abstract.....	13
2.2. Introduction.....	14
2.3. Experimental details .....	16
2.4. Results and discussion.....	18
2.5. Conclusions.....	22
References.....	23
Figures.....	25
3. Conclusions.....	30

## LIST OF FIGURES

<u>Figure</u>	<u>Page</u>
2.1 X-Ray diffraction patterns for thin-films annealed at different temperatures.....	25
2.2 Atomic force microscope images of annealed films with resulting RMS and z-ranges.....	25
2.3 X-Ray reflectivity measurements at low angles.....	26
2.4 Fourier transform infrared spectra of films.....	26
2.5 Refractivity properties of standard solution deposition.....	27
2.6 Thickness vs. concentration of solution study.....	27
2.7 Refractive properties of low concentration precursors.....	28
2.8 Flow Diagram for precursor preparation.....	28

## LIST OF TABLES

<u>Table</u>	<u>Page</u>
2.1 Model fitting output for deposited films.....	29

Con todo mi cariño para mi familia,

(With all my love to my family)

Thin-Film Dielectric Structure and Performance of  
Spin-Coated ZrO<sub>2</sub> from Aqueous Inorganic Solution

**CHAPTER 1: INTRODUCTION**

## 1.1 Current Status of high-k dielectrics

Throughout the history of chemistry, the structure of metal oxides in different environments has been studied, from the most essential quantum calculations to more experimental approaches like synthesis. The scope of synthesis itself entails many fields, from the extraction of raw materials in mineralogy to the engineering of their respective applications. Metal oxides form part of our everyday lives from the very niche of the home to the more visited places we populate throughout our existence. Many of the metal oxides that have become essential parts of our society begin as mere curiosities, transformed through years of research. While some metal oxides can be extracted from rich ores, others can only be synthesized in laboratory spaces. Some metal oxides have never been synthesized due to physical constraints and are only part of our theoretical studies in order to confirm the instabilities of the system. These factors make synthesis methods very important applications, at the core of materials chemistry.

Crystal structures of metal oxides can be intriguing to decipher, and may vary a great deal despite similar building blocks. In the past, many formulas of oxides were merely guessed until the use of crystal x-ray diffraction, through which many of these formulas became exact. With the introduction of metal oxides thin films into the electronics industry, major advancements have been made. Many of these require thin films to be

amorphous, rather than crystalline, due to better electrical properties. In an amorphous state, the crystal structure of the thin-film can't be known, although some attempts have been made by Chris Knutson to determine in fact whether or not amorphous thin-films deposited from aqueous precursors are as disordered as we tend to think. These types of studies will further help to find structure for many of these amorphous metal oxides, and even predict coordination changes as an amorphous material becomes crystalline.

The introduction of metal oxides in electronics has yielded promising results. The introduction of SiO<sub>2</sub> in metal-oxide semiconductors (CMOS) revolutionized the technologies market and rapidly expanded its applications. Mainly due to CMOS performance (speed), low static (off-state) power, and a wide range of power supply and output voltages.<sup>2</sup>

$$C_{ox} = \frac{\kappa\epsilon_0 A}{t_{ox}} \quad (1)$$

As technology market has demanded performance, devices have scale down. However, this has an impact on thin film layers. Eq. 1 determines the capacitance of a simple parallel plate capacitor. As the thickness of the dielectric (d), decreases, the capacitance (C) of the device increases; however, ultrathin SiO<sub>2</sub> properties, such as tunneling, create limitations to the reliability of these electronics at low thicknesses. Due to these limitations, many researchers (including us) have looked at materials

with high dielectric constants ( $k$ ), in order to maintain a thickness through which electrons will not tunnel. For this discussion, we limited ourselves to only discussing Group IVB binary metal oxides ( $\text{TiO}_2$ ,  $\text{ZrO}_2$ , and  $\text{HfO}_2$ ), with experimentation only concerning  $\text{ZrO}_2$  in Ch 2.

## 1.2 Group IVB Metal Oxide Thin Films

The application of Group IV metal oxides in electronics has yielded promising results as an alternative to  $\text{SiO}_2$ . The platform for these alternatives, especially from aqueous inorganic precursors, is quite challenging mainly because of the complex hydrolysis and condensation behaviors of active metals. Therefore dielectric materials from inorganic aqueous precursors need comprehensive studies. It is known that a reliable dielectric layer plays a key role in a high performance thin film transistor<sup>2</sup>. As a dielectric layer, must be free of major defects and dense in order to decrease current leakage. An excellent review of high-dielectric written by Wilk and Wallace<sup>1</sup> offers a review of the current situation of most high- $\kappa$  dielectrics covering different types of deposition methods. In this work, we consider group IVB metal oxides use as a high- $\kappa$  type dielectric.

Applications of  $\text{TiO}_2$  often receive the most attention because  $\text{TiO}_2$  exhibits a high dielectric constant of 80-110.<sup>1</sup>  $\text{HfO}_2$  has also been used as



an alternative high-k dielectric layer in thin film transistors (reference Aoki .et.). Jiang and others developed solution processing methods for both  $\text{TiO}_2$  and  $\text{HfO}_2$  thin-film deposition.<sup>3,4</sup> For aqueous solution deposited  $\text{TiO}_2$ , thin films show high density and an overall good morphology in both the amorphous and crystalline phases. The deposition of  $\text{HfO}_2$  from aqueous precursors in ambient conditions has been an enormous development for alternative electronic materials. Jiang showed excellent electronics results with MIM test structures and TFTs. It is upon this model that our research with  $\text{ZrO}_2$  was based. The similar chemistries of Zr and Hf make Jiang's work with  $\text{HfO}_2$  strongly relevant to ours.

### **1.3 Thin Film Deposition Methods**

In order to make rationale for using aqueous solution processing clear, a brief summary of metal oxide deposition methods will be made, from a chemist's point of view. Discussion will include some of the main deposition systems, such as thermal evaporation, sputtering, atomic layer deposition (ALD), chemical vapor deposition (CVD), and chemical solution deposition (chemical bath deposition, and spin-coating). Ideally, a deposition system should be energy efficient, should not produce harmful byproducts, and most importantly, should produce good quality thin-films that are smooth, dense, and free of major defects.

Thermal evaporation is a process in which a material is heated until it changes to the gas phase and deposits onto a substrate. Current passes through tungsten until enough heat is released. This takes place in a low-pressure chamber where the mean free path distance is longer than the distance between the source and the substrate and thus a uniform layer can be deposited. Among the metals that can be deposited by this method are Ti, Au, Ni, Al, and SnO<sub>2</sub>. Thermal evaporation deposition is often used to deposit Al contacts (for electronic testing and characterization) onto a substrate in a substrate-metal-insulator-metal stack (also known as MIM).

Sputtering is a very convenient method where a ceramic or a metal target is bombarded with plasma thereby ejecting particles that travel through the chamber and deposit onto the substrate. Using glow discharge between the target and the substrate generated collisions from energetic ions, such as Ar<sup>+</sup>. Gases can be introduced into the chamber such that these gases are incorporated into the final sputtered film. Among these gases, O<sub>2</sub> is used in the deposition of metal oxides. As with thermal evaporation, the chamber where the deposition is done is in low pressure to increase the mean free path, resulting in uniformly deposited thin-films<sup>2</sup>. With this method there is often a silicate interface layer formed between the *n*-type Si and ZrO<sub>2</sub>.<sup>5</sup> This layer can be found by using x-ray

photoelectron spectroscopy (XPS). There have been some studies where the use of a substrate bias can result in thinner interfacial layer.<sup>6</sup>

Chemical vapor deposition is a standard procedure to deposit many compounds from non-metallic to intermetallic compounds. The compound is deposited from a chemical reaction in the vapor phase. Several applications of CVD technology have been implemented successfully such as metallo-organic CVD, plasma CVD, laser CVD and others. Its versatility of coverage over large areas and any topography has made it possible to use in many applications. The main limitation to this deposition system is that the deposition is most versatile at high temperatures where the substrate stability is limited. In flexible substrate applications, for example, substrates remain stable to temperatures of only about 300 °C. Another limitation is the usage of high vapor pressure precursors that are hazardous and toxic for the environment.<sup>9</sup> Toxic byproducts must be neutralized for discharge, which adds to the cost of the procedure.

One specialization of CVD that offers a way to synthesize novel thin-films is atomic layer deposition (ALD). It is known for offering precision over the thickness deposited, excellent coverage per cycle, and dense films. The main method for depositing a film is to cycle precursor gases that

react on the chamber and are deposited on the film one layer at a time. This monolayer deposition method results in a slow deposition system. A deposition done by Cassir and Goubin<sup>7</sup> yielded a maximum monolayer cycle of 0.5nm for  $ZrO_2$ . After one layer is deposited the chamber is usually purged on remaining gases prior to the next cycle. For this reason, depositing high thicknesses can be time consuming. Another challenge that this system has is the temperature that the deposition has to be made under. This temperature is proportional to that needed to promote bonding in the chamber. This deposition temperature can lead to changes from amorphous films to crystalline which is undesirable for many high-performance dielectric platforms. Another downside to this deposition system is the use of organic precursor. One precursor type, alkylamines, has low deposition cycles as much as 0.096 nm and 0.093 nm for  $ZrO_2$  and  $HfO_2$  respectively.<sup>8</sup>

From these deposition systems is where we will try to improve upon. The development of precursors is often a tactic taken, and a route that deviates without the use expensive vacuum systems. As with these deposition systems require high energy for the deposition of films and/or lithography is used as part of the electronic making process. In solution processing, different advantages are present like having control over morphologies, densities, and precise control over thicknesses by studying

the precursor system. Intricate variables, for example, can be the addition of an acid that can either aid a metal compound to go into solution or displace a ligand and form part of the metal complex (this can occur if the overall energy of the compound decreases as it replaces the other coordination for the  $A^-$  of the acid-HA). Two categories of chemical solution deposition will be cover: CBD and spin-coating.

Chemical bath deposition is a very traditional way to coat a substrate for a specific period of time and obtain thin-films. The deposition of the film is usually done at room temperature. Among the many of the materials that can be successfully deposit are semiconductors like CdS, CdSe, and ZnS. For a CdS film, a salt of cadmium (i.e.  $CdCl_2$ ) is dissolved in a high pH environment where sulfide ions are present; CdS will cover a submerged substrate. Like CVD, CBD can coat any substrate in a 2-D or 3-D manner. The limiting factor for the thickness of the film is the amount of reactants available (for CdS either the salt or the sulfide can be used for the limiting reactant). It is from CBD that spin coating was developed, from a transitional “dropper” method that eventually evolved into spin coating.

Spin coating uses a precursor synthesis much like CBD but without the soaking required of a substrate for prolonged periods of time. Unlike the

dropper method, spin-coating provides a route to reproducible results. Precursor development is the most important part of spin coating deposition. During the development, the aqueous chemistry of Zr was used to determine a route to make a final nitrate-peroxide based precursor. A characteristic of the metal in solution is that it must be stable enough to hydrolyze in the precursor and condense during spinning, but not so stable that the metal oxide will precipitate out of solution. It is from these guidelines that the precursor synthesis was developed (a more detail explanation is offered in Ch.2 under precursor chemistry). The solution is deposited on the substrate via syringe. Excess of solution is spun out at 3000 rpm, which also helps the distribution of the film. After the spinning of the substrate for 30 s, the substrate is densified and dehydrated at a chosen temperature unique to each precursor

#### **1.4 Summary**

It is from this platform that we intend to make the case for  $\text{ZrO}_2$  in the manufacturing of smooth, dense, cost effective, environmentally friendly materials. Understanding the aqueous solution chemistry is the key for synthesis of nitrate-based precursors. The following chapter will go in detail for methods taken for this development.

## References

1. G.D. Wilk, R.M. Wallace, J.M. Anthony. *J. App. Phys.* 89 (2009), 10, 5243-5275
2. C.L. Munsee, M.S. Dissertation, Oregon State University, 2005
3. K. Jiang, A. Zakutayev, J. Stowers, M.D. Anderson, *Solid State Sciences*, 11 (2009), 1692-1699
4. K. Jiang, J.T. Anderson, K. Hoshino, D. Li, J.F. Wager, D.A. Keszler. *Chem. Mater.* 23 (2011) 945-952.
5. J. Zhu, Z.G. Liu. *Applied Physics A* 78 (2004), 741-744
6. A. P. Huang, P.K. Chu, *Materials Science and Engineering*, B 121 (2005), 244-247
7. M.Cassir, F. Goubin, C. Bernay, *Applied Surface Science*, 193 (2002), 120-128
8. D. M. Hausman, E. Jim, J. Becker, *Chem. Mater.* 14 (2002), 4350-4358

**CHAPTER 2: AQUEOUS SOLUTION CHEMISTRIES OF SOLUTION  
DEPOSITED ZIRCONIUM (IV) OXIDE**

Hidekel A. Moreno Luna, Sharon Betterton, Douglas Keszler



## 2.1 Abstract

An aqueous peroxo-zirconium precursor has been developed for the deposition of amorphous and crystalline  $\text{ZrO}_2$  via spin-coating. Deposition using a 0.2 M  $[\text{Zr}^{4+}]$  precursor yields thin films at 6-7 nm per coat after a modest anneal temperature of 150 °C. Films annealed at selected temperature (between 150 °C and 800 °C) demonstrate low roughness (0.2-1.7 nm RMS) when analyzed by atomic force microscopy (AFM), confirmed by X-ray reflectivity (XRR) analysis. Densities as high as 5.11 g/cm<sup>3</sup> (90% bulk) were determined from XRR for films annealed at 300 °C, and densities for all films were calculated from refractive index values to be between 87% and 89% of bulk. These films also exhibit  $n(\lambda = 550 \text{ nm}) = 1.97$  at 300 °C. Furthermore, ultra-thin films <10 nm have been deposited by diluting a standard solution, demonstrating an easily tunable means of depositing  $\text{ZrO}_2$  at a desired thickness. A window temperature for MIM making was found to be 350-500 °C from IR spectroscopy and X-ray diffraction (XRD).

## 2.2 Introduction

High-permittivity metal oxides such as  $\text{ZrO}_2$ ,  $\text{HfO}_2$ , and  $\text{Ta}_2\text{O}_5$  are attractive candidates for gate dielectric materials across a wide range of high-performance thin-film transistor platforms.<sup>1</sup> These materials are under consideration as potential replacements for  $\text{SiO}_2$ , with which high current leakage is observed at low thicknesses. Hafnium and zirconium oxides have received considerable attention for their high dielectric constants and electrical performance.<sup>1-4</sup>  $\text{ZrO}_2$  and  $\text{HfO}_2$  films deposited by using atomic layer deposition (ALD) methods exhibit dielectric constants ranging from 20-29 and 16.3-18.5, respectively<sup>5</sup> more than four times that exhibited by  $\text{SiO}_2$ . Zirconia, both amorphous and crystalline, has been deposited using many methods: sputtering,<sup>6</sup> pulse layer deposition,<sup>2</sup> CVD,<sup>7</sup> liquid-phase deposition,<sup>8</sup> successive ionic layer absorption and reaction,<sup>9</sup> and ALD.<sup>4,10</sup>

Though the development of high- $\kappa$  dielectrics has gained significant attention, deposition of high- $\kappa$  metal oxides by solution-based methods is often neglected, in part due to concerns about moisture incorporation, which can result in sharp increases in conductivity<sup>10</sup> and also because of difficulties in obtaining desired film morphologies. For thin-film dielectrics to be considered appropriate for use in electrical applications, films must be smooth, dense, and free of major defects.<sup>1</sup>

While organic solution deposition methods typically seek to resolve moisture issues by replacing water with organics (such as metal amides<sup>5</sup>),

this resolution is problematic because of the high annealing temperatures required to remove residual organics, which can result in inhomogeneous, rough, and low-density films.

We shift our attentions away from the pitfalls of organic solution deposition by utilizing aqueous, inorganic solution deposition, which combats both moisture incorporation (through a dehydration step) and density issues (by making use of small, inorganic ligands that do not require high annealing temperatures). Deposition of oxide thin films from aqueous precursors, specifically via spin-coating, is a technique that has yielded promising results with regard to the incorporation of metal oxides (e.g.  $\text{HfO}_2$ ,<sup>11</sup>  $\text{ZnO}$ ,<sup>12</sup>  $\text{Al}_2\text{O}_3$ ,  $3x(\text{PO}_4)_{2x}$ ,<sup>13</sup> and  $(\text{InGaZn})_x\text{O}_y$ <sup>14</sup>) into electronic applications.

The deposition and characterization of  $\text{HfO}_2$  and  $\text{ZrO}_2$  is often a dual investigation due to their similar chemistries. This work seeks to expand upon others' research<sup>11</sup> on the deposition of  $\text{HfO}_2$  by focusing on the aqueous, inorganic deposition, and subsequent characterization, of  $\text{ZrO}_2$  thin films. A similar study was done by Jiang and Anderson, in which they used a peroxo-hafnium complex precursor solution to deposit high quality  $\text{HfO}_2$  thin films via spin-coating.<sup>11</sup> Gao and Masuda likewise attempted a similar study: using a peroxo-zirconium solution, based on the  $\text{ZrO}(\text{NO}_3)_2$  complex, they were able to deposit  $\text{ZrO}_2$  on p-type Si wafers using a chemical bath method. However, their resulting solutions were unstable at room temperature and had a stability window that restricted deposition.<sup>8</sup> Notable advantages of our

precursor synthesis are the reasonable stability of the precursor, as well as the elimination of ammonia, which can raise the dehydration temperature of the deposited films.

## 2.3 Experimental Details

*2.3.1 Preparation of Precursor Solution and Thin Film Deposition.*  $\text{ZrOCl}_2 \cdot 8\text{H}_2\text{O}$  (Alfa Aesar, 99+%) was dissolved in 18.2-M $\Omega$  Millipore  $\text{H}_2\text{O}$  to a concentration of 0.5 M. This stock solution was further diluted to desired concentrations with 18.2-M $\Omega$   $\text{H}_2\text{O}$ . As a representative solution, 0.5 M  $\text{ZrOCl}_2(\text{aq})$  was diluted to 20 mL in order to obtain a 0.12 M solution. To this 20 mL solution, 6.7 mL of 1 M  $\text{NH}_3(\text{aq})$  (Mallinckrodt, ACS) was added and vigorously stirred. The resultant precipitate was centrifuged and then washed with  $\text{H}_2\text{O}$  a total of 5 times to remove  $\text{Cl}^-$  and  $\text{NH}_3$ . After the final decant, 1.4 mL 2 M  $\text{HNO}_3$  (EDS, ACS) and 2.5 mL 30%.wt  $\text{H}_2\text{O}_2(\text{aq})$  (Mallinckrodt, ACS) were added. This final solution was stirred for 12 h until clear and chilled prior to deposition.

*2.3.2 Thin Film Deposition.* Thin films were deposited via spin-coating. Precursors were filtered through a 0.45 $\mu\text{m}$  PTFE syringe filter onto a substrate and then spun at 3000 rpm for 30 s, followed by a 150  $^\circ\text{C}$  cure for 60 s and a 20 s cooling step. This process was repeated until the desired thickness was achieved. For a 0.2 M  $[\text{Zr}^{4+}]$  solution, the deposition cycle produced a 6-7 nm layer, dependent on synthesis yield; for an 85%  $[\text{Zr}^{4+}]$

yield, the layer thickness per deposition cycle was 6.6 nm. Films were annealed in air for 1 h at temperatures ranging from 200°C to 800 °C. Substrates (200 nm SiO<sub>2</sub> thermally grown on Si) were prepared by sonicating substrates for 60 min in a 5% Contrad 70 solution at 45 °C and then thoroughly rinsing with 18.2-MΩ Millipore H<sub>2</sub>O.

*2.3.3 Structural Characterization.* Diffraction data of deposited thin films were collected on a Rigaku RAPID diffractometer. Thin-film-surface-morphology was analyzed by using a Digital Instruments NanoScope III Multimode atomic force microscope (AFM) in contact mode operation with a Veeco NP-20 SiN<sub>x</sub> probe and a scan rate of 1.5 Hz. X-ray reflectivity (XRR) measurements were collected on a Rigaku Ultima IV X-Ray diffractometer equipped with Cu K $\alpha$  radiation. Reflectivity was measured from 0-10 ° (2 $\theta$ ) and roughness, thickness, and density analyses were deduced by simulating the reflection pattern using the GlobalFit Reflectivity Program. Transmission Fourier transform infrared (FT-IR) spectra of a thick film as a function of annealing temperature was also measured in a Nicolet 5PC spectrometer. Data were analyzed by the OMNIC program.

*2.3.4 Optical Characterization.* Film thicknesses and indices of refraction of ZrO<sub>2</sub> thin films were measured by using a J.A. Woollam HS-190 Ellipsometer. Incident angles used were 65-75 ° with 5 ° steps from 300 nm to 800 nm. VASE software was used to model measured data. Data were fit using the Cauchy model for a ZrO<sub>2</sub> layer. Table 1 shows the parameters:

anneal temperature ( $^{\circ}\text{C}$ ), precursor concentration ( $M$ ), film thickness ( $\text{nm}$ ), Cauchy parameters  $A$ ,  $B$ , and  $C$  for dispersion ( $n(\lambda) = A + B/\lambda^2 + C/\lambda^4$ ) in the  $\text{ZrO}_2$  layer, and mean square error ( $MSE$ ).

## 2.4 Results and Discussion

*2.4.1 Thin Film Deposition and Characterization.* As shown by XRD (Figure 2.1) first sign of the monoclinic  $\text{ZrO}_2$  phase appears at  $400\text{ }^{\circ}\text{C}$ . By  $500\text{ }^{\circ}\text{C}$  the film is crystallized completely in the monoclinic phase. Below  $400\text{ }^{\circ}\text{C}$  the film appears to be amorphous.

Root-mean-square (RMS) roughness values were calculated via contact-mode AFM in order to determine the roughness of thin films as a function of temperature. At lower anneal temperatures;  $\text{ZrO}_2$  thin films demonstrate low roughness, which increases at higher annealing temperatures as shown in Figure 2.2. RMS roughness values from AFM scans ranged from  $0.2\text{ nm}$  to  $1.7\text{ nm}$ , with values  $<0.4\text{ nm}$  for anneal temperatures  $500\text{ }^{\circ}\text{C}$  and below. Reflectivity measurements of the film at low incident angles are provided in Figure 2.1. The modeled data show low roughness values at both non-crystalline and crystalline phases with values between  $0.01\text{ nm}$  and  $0.02\text{ nm}$  for films that were  $41.96\text{ nm}$ ,  $41.42\text{ nm}$ , and  $42.53\text{ nm}$  thick and annealed at  $300\text{ }^{\circ}\text{C}$ ,  $500\text{ }^{\circ}\text{C}$ , and  $700\text{ }^{\circ}\text{C}$ , respectively. Shown is the reflected X-ray intensity  $\log(I)$  of the annealed films as a function of incident X-ray angle.

Densities of the annealed films, also determined by using XRR, decrease with annealing temperatures: At  $300\text{ }^{\circ}\text{C}$ , a film with a thickness of  $\sim 41\text{ nm}$

and a roughness value of 0.015 nm had a density of 5.11 g/cm<sup>3</sup> – reasonably close to the bulk density given by Wood and Nassau (5.68 g/cm<sup>3</sup>).<sup>15</sup> This confirms that high densities of deposited ZrO<sub>2</sub> thin films can be realized by modest annealing temperatures.

Transmittance FT-IR spectrum of a thick film (200-250nm) is shown in Figure 2.4. O-H stretches, located at 3500cm<sup>-1</sup>, are present at 150 °C and 250 °C, meaning that the film is not completely dehydrated at these temperatures, while after annealed at 350 °C, this peak is indiscernible. As moisture incorporation in the film will result in high loss tangent, tanδ, the ideal temperature to anneal ZrO<sub>2</sub> thin films for use in metal-insulator-metal test devices is 350 °C.

The refractive indices of crystalline films were found to be lower than those of amorphous films (see Figure 2.5 for representative films). At 550 nm, the refractive index for a 300 °C annealed film is 1.97, while at 700 °C it is 1.95. These values are close to that of the bulk material at 550 nm,  $n = 2.17$ .<sup>15</sup>

The refractive index can also be used to estimate the density of the films, allowing for comparison with XRR results. This relationship is described by:

$$\frac{\rho_f}{\rho_m} = \left( \frac{n_f^2 - 1}{n_f^2 + 2} \right) \left( \frac{n_m^2 + 2}{n_m^2 - 1} \right) \quad (2)$$

where  $n_f$  is the refractive index of the film,  $n_m$  is the refractive index of the bulk material,  $\rho_f$  is the density of the film, and  $\rho_m$  is the density of the bulk

material.<sup>16</sup> Using this equation, estimated densities were calculated to be between 87% and 89% of bulk for films annealed between 300 °C and 700 °C, a value of  $\sim 5.00 \text{ g/cm}^3$  at 300 °C. At this temperature, a value of  $5.11 \text{ g/cm}^3$  was measured by XRR.

Ultra-thin films <10nm were also made by diluting the standard concentration and depositing diluted precursor solutions. Average thicknesses per deposition cycle were found for 0.035–0.200 M  $[\text{Zr}^{4+}]$  by depositing 5 layers of  $\text{ZrO}_2$  and dividing measured thicknesses by 5 (see Figure 2.6); a second order relationship is clear, demonstrating the ability to control the layer thicknesses precisely. The minimum thickness per cycle experimentally achieved was 1.02(8) nm per deposition cycle, at 0.035 M  $[\text{Zr}^{4+}]$ .

Thinner films demonstrated typical refractive properties compared with those for thicker films, as shown in Figure 2.7. A thinner film (6 nm) annealed at 150 °C exhibited  $n(\lambda = 300 \text{ nm}) = 2.6$ , whereas a thicker film (22.5 nm) annealed at 150 °C had  $n(\lambda = 300 \text{ nm}) = 2.1$ . This behavior suggests a higher density of the film at lower thicknesses, which is reasonable because a thinner film has more tendency to densify at lower temperatures.

*2.4.2 Precursor Chemistry.* The overall reaction and products have been shown in Figure 2.1 as a flow chart of the precursor synthesis. Upon dissolution of  $\text{ZrOCl}_2 \cdot 8\text{H}_2\text{O}$  (an ionic cluster containing  $[\text{Zr}_4(\mu-$



$(\text{OH})_8(\text{H}_2\text{O})_{16}]^{8+}]^{17}$  in water, the tetrameric cation has been determined by others<sup>18</sup> to be preserved, though subsequent polymerization is dependent on pH (changes in pH can often lead to different conformations around  $\text{Zr}^{4+}$ ), aging temperature, and concentration of the solution.<sup>19</sup>

In Step 2, ammonia is added, raising the pH considerably. This leads to the formation of a hydrous zirconia precipitate through ololation and oxolation of the previously described tetramers. The nature of this hydrous zirconia is described by Clearfield<sup>20</sup> as an anhydrous  $\text{ZrO}_2$  core, with each metal cation coordinated to eight oxygens (themselves coordinated to four  $\text{Zr}^{4+}$  cations), terminated by protonated oxygens. These terminal surface oxygens, in the form of hydroxo groups and water molecules, terminates the oxolation processes and prevents the further growth of zirconia particles.

Washing steps, designed to remove ammonia and chloride, are necessary for film quality. To assure that the unwanted ionic species were fully washed from the precipitate, decanted supernatants from wash steps were tested with  $\text{AgNO}_3$  (aq) until no precipitations were formed.

The addition of  $\text{HNO}_3$  to the final, washed precipitate allows the dissolution of the precipitate without the destruction of polymeric species (Step 3). Because of the weak bonding of  $\text{NO}_3^-$  to the Zr complex, dehydration is then possible with low temperature curing steps.

The addition of  $\text{H}_2\text{O}_2$  in Step 4 improves the dissolution time of the precipitate in  $\text{HNO}_3$  and has other benefits, as well.<sup>19</sup> The presence of peroxy

ligands in the solution prevent premature condensation by replacing hydroxo bridges and ultimately lower the film curing temperature because they are easily decomposed.

## **2.5 Conclusions**

Dense, and smooth  $\text{ZrO}_2$  thin films that are free of major defects have been deposited by using a nitrate based peroxo-zirconium precursor via spin-coating deposition. Deposited films show densities as high as 90% of the bulk density. Films further demonstrate high refractive properties at annealing temperatures as low as 150 °C. Above 350 °C water incorporation is minimized, and below 500 °C the films are amorphous; therefore the ideal temperature range for these in terms of device applications is 350 °C-500 °C. Ultra-thin films were prepared by diluting standard solutions, demonstrating one of the unique advantages over traditional methods: precise control of metal oxide thickness without the need for expensive vacuum systems.

## References

1. G.D. Wilk, R.M. Wallace, J.M. Anthony. *J. Appl. Phys.* 89 (2001) 5243-5275.
2. C.H. Lee, H.F. Luan, W.P. Bai, S.J. Lee, T.S. Jeon, Y. Senzaki, D. Roberts, D.L. Kwong. *IEDM.* (2000) 27-30.
3. L. Zhong, Z. Zhang, S.A. Campbell, W.L. Gladfelter. *J. Mater. Chem.* 14 (2004) 3203-3209.
4. D.H. Hausmann, E. Kim, J. Becker, R.G. Gordon. *Chem. Mater.* 14 (2002) 4350-4358.
5. M.J. Biercuk, D.J. Monsma, C.M. Marcus, J.S. Becker, R.G. Gordon. *Appl. Phys. Lett.*, 83 (2003) 2405-2407.
6. L.Q. Zhu, Q. Fang, G. He, M. Liu, L.D. Zhang. *Nanotechnology.* 16 (2005) 2865-2869.
7. Y. Gao, Y. Masuda, H. Ohta, K. Koumoto. *Chem. Mater.* 16 (2004) 2615-2622.
8. S. Park, B.L. Clark, D.A. Keszler, J.P. Bender, J.F. Wager, T.A. Reynolds, G.S. Herman. *Science.* 297 (2002) 65.
9. M. Cassir, F. Goubin, C. Bernay, P. Vernoux, D. Lincot. *Appl. Surf. Sci.* 193 (2002) 120-128.
10. C. Munsee. M.S. Dissertation, Oregon State University, 2005.
11. K. Jiang, J.T. Anderson, K. Hoshino, D. Li, J.F. Wager, D.A. Keszler. *Chem. Mater.* 23 (2011) 945-952.
12. S.T. Meyers, J.T. Anderson, C.M. Hung, J. Thompson, J.F. Wager, D.A. Keszler. *J. Am. Chem. Soc.* 130 (2008) 17603-17609.
13. S.T. Meyers, J.T. Anderson, D. Hong, C.M. Hung, J.F. Wager, D.A. Keszler. *Chem. Mater.* 19 (2007) 4023-4029.
14. G.H. Kim, H.S. Shin, B.D. Ahn, K.H. Kim, W.J. Park, H.J. Kim. *J. Electrochem. Soc.* 156 (2009) H7-H9.

15. J. Adam, M. D. Rogers. *Acta Crystallogr.* 12 (1959) 951.
16. R.E. Klinger, C.K. Carniglia. *Appl. Opt.* 24 (1985) 3184-3187.
17. Y. Liu, P.H. Daum. *J. Aerosol. Sci.* 39 (2008) 974-986.
18. M. Nakayama, A. Sato, K. Ishihara, H. Yamamoto. *Adv. Synth. Catal.* 346 (2004) 1275-1279.
19. N. Rao, M.N. Holerca, M.L. Klein, V. Pophristic. *J. Phys. Chem. A.* 111 (2007) 11395-11399.
20. A. Clearfield, P.A. Vaughan. *Acta Crystallogr.* 9 (1956) 555-558.
21. A. Clearfield. *Chem. Rev.* 88 (1988) 125-148.

## Figures

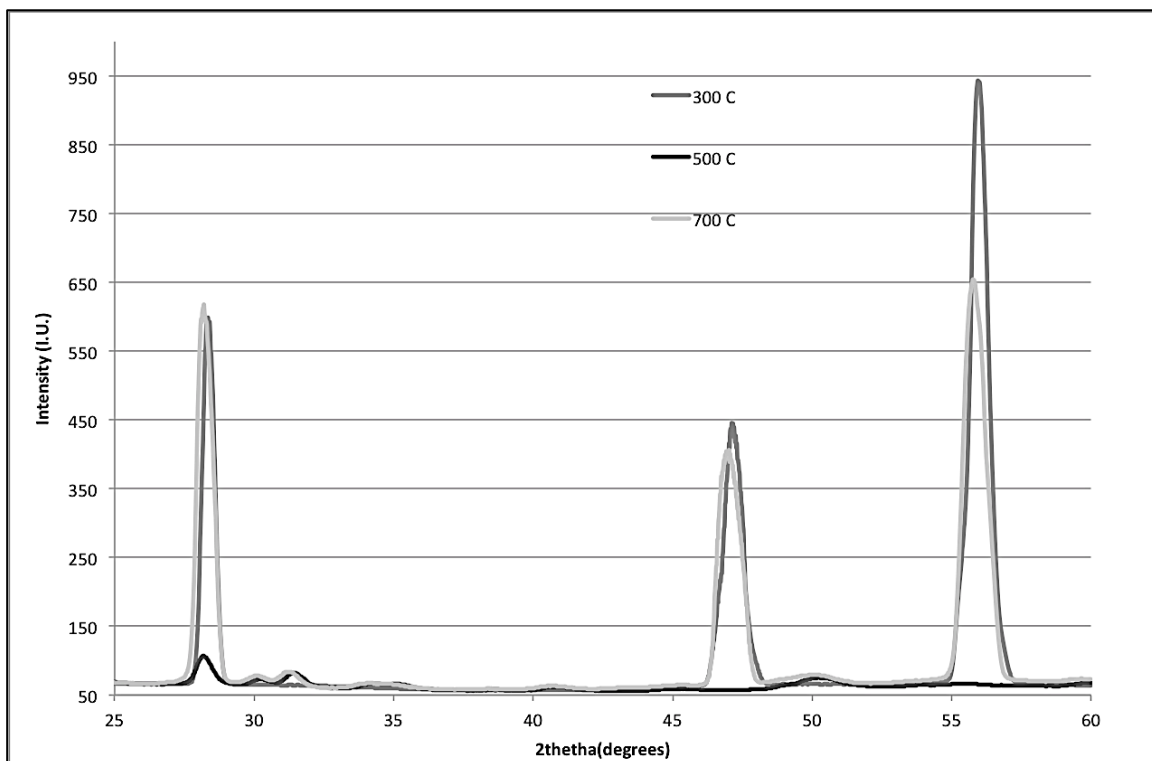


**Figure 2.1** XRD patterns for representative annealing temperature

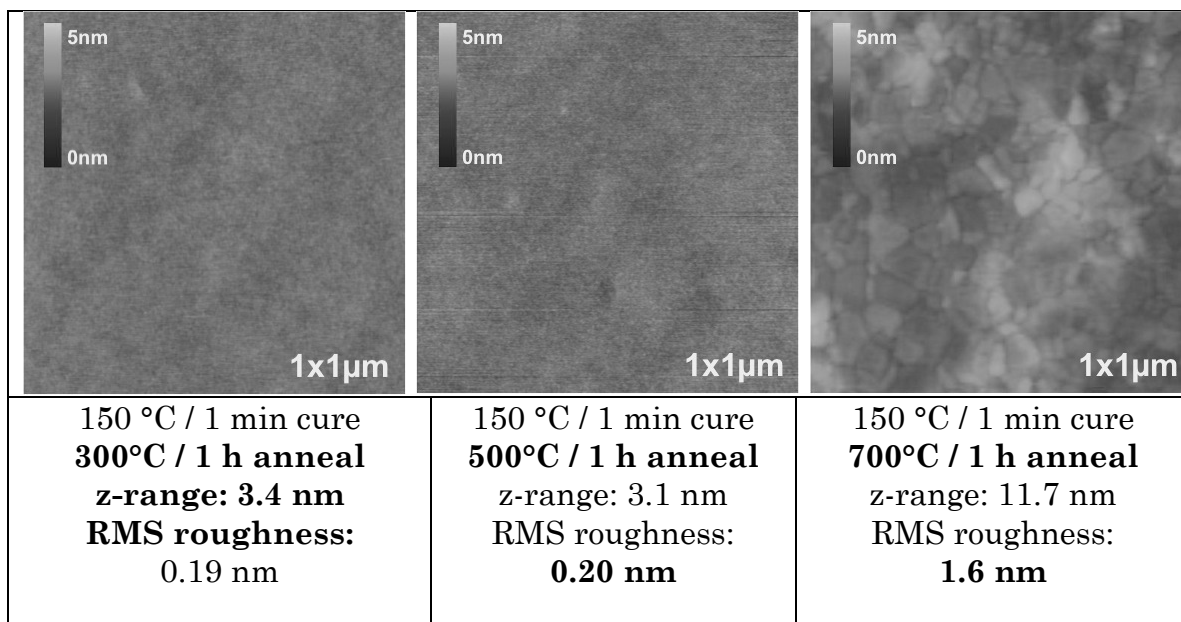


**Figure 2.2** Atomic force microscope images according to their annealing temperature

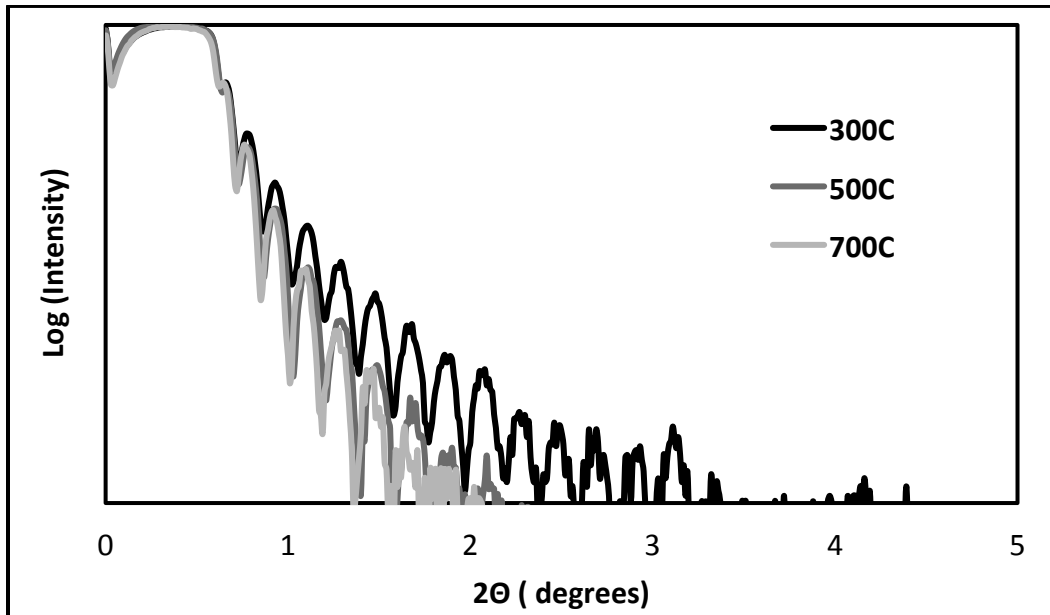


**Figure 2.3** X-Ray reflectivity measurements at low incident angles for  $ZrO_2$  thin films annealed 1 h at varying temperatures

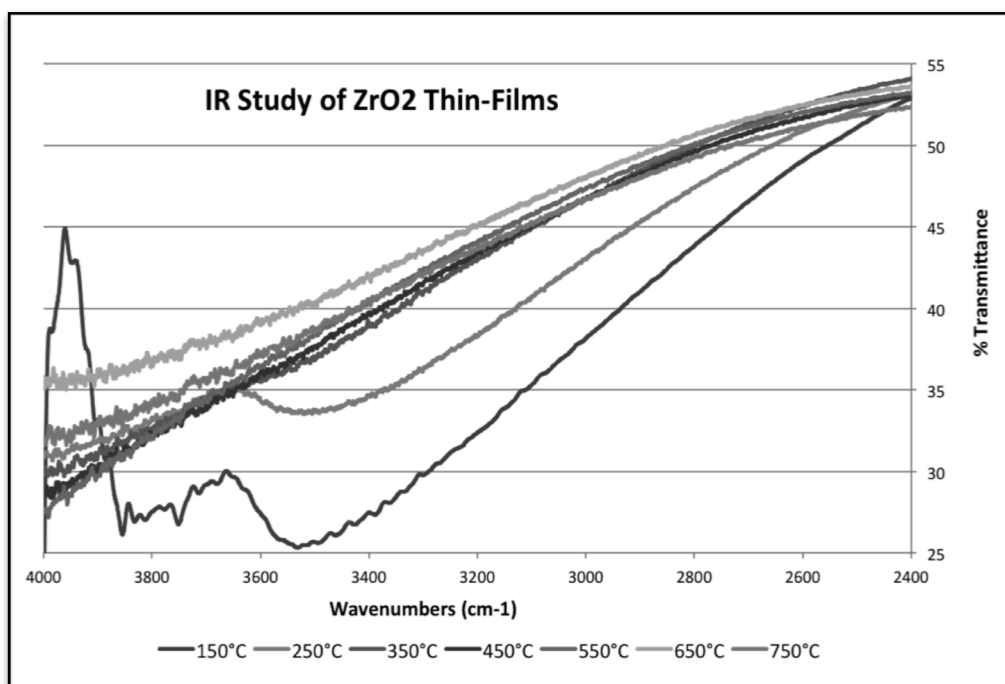


**Figure 2.4** IR transmission spectra of  $ZrO_2$  for 150-750 °C annealing temperatures

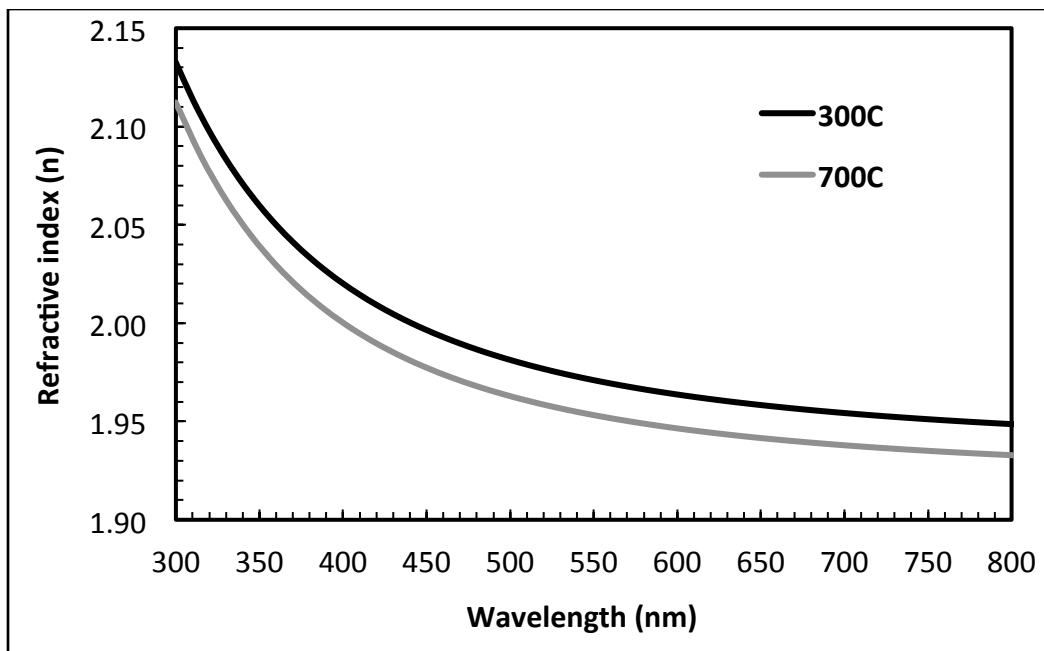


**Figure 2.5:** Refractive index vs. wavelength for  $\text{ZrO}_2$  thin films deposited from 0.2 M precursor at two representative anneals.

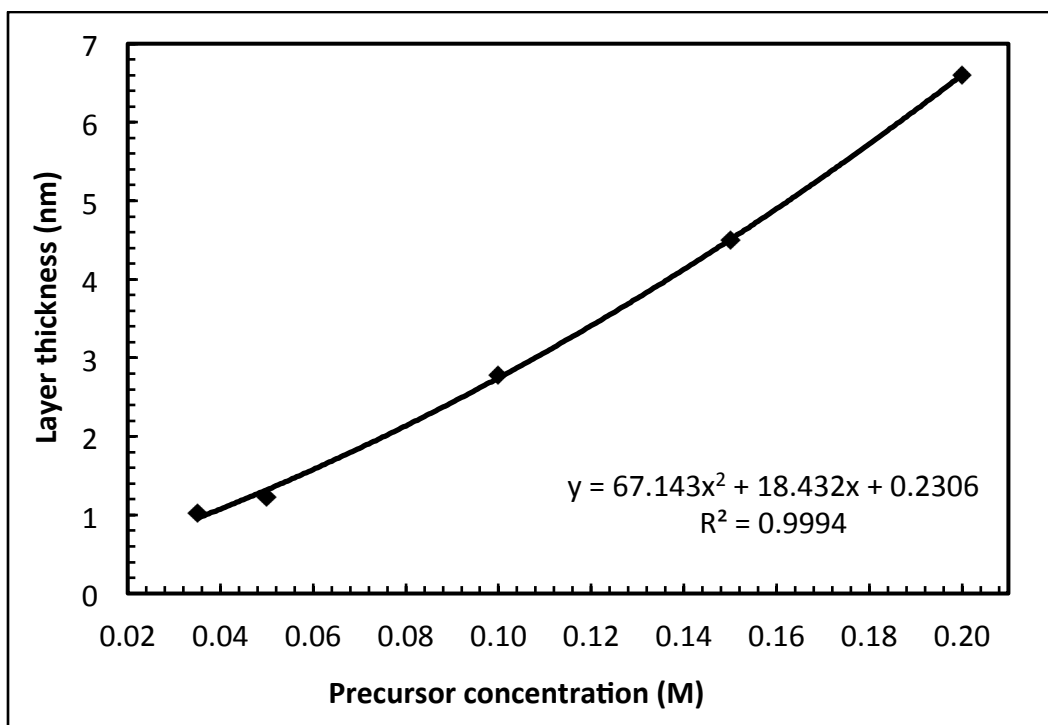


**Figure 2.6**  $\text{ZrO}_2$  thin film thickness vs. precursor concentration. Points calculated by depositing 5 layers at 150 °C for 1 h and then dividing by 5.

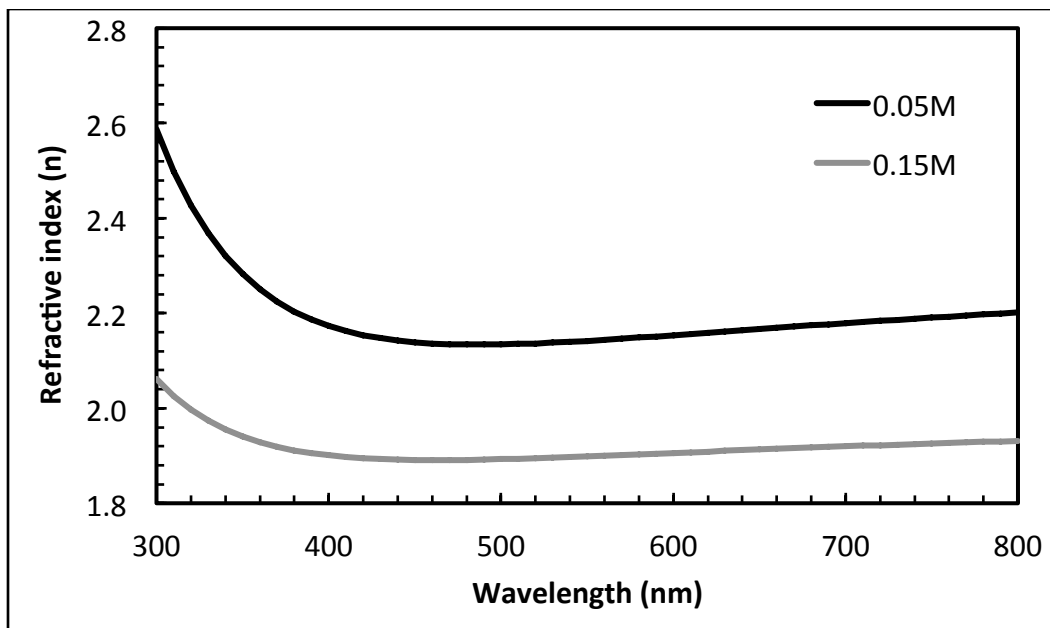


**Figure 2.7** Refractive index vs.  $\lambda$  for  $\text{ZrO}_2$  thin films deposited from lower concentration precursors and annealed at  $150\text{ }^\circ\text{C}$ .

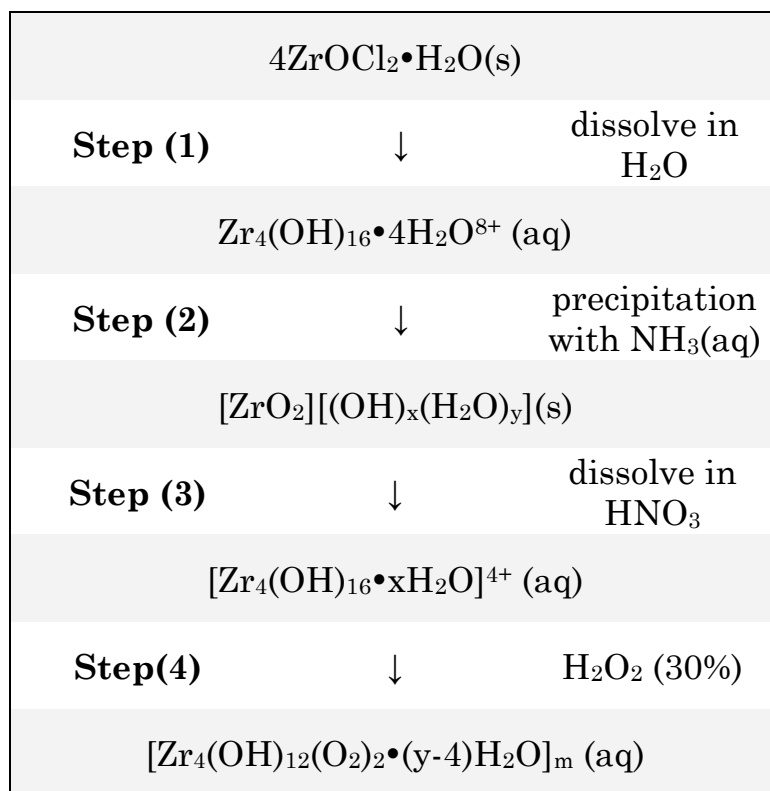


**Figure 2.8** Flow diagram for the preparation of  $\text{ZrO}_2$  precursor.



**Table 2.1** Model fitting results for  $\text{ZrO}_2$  thickness, Cauchy parameters A, B, and C, and mean square error (MSE).

Anneal (°C)	$[\text{Zr}^{4+}]$ (M)	$t$ ( $\text{ZrO}_2$ ) (nm)	$A$	$B$	$C$	$MSE$
300	0.20	231.7(4)	1.932(2)	$8.79(65) \times 10^{-3}$	$8.26(5) \times 10^{-4}$	15.43
700	0.20	210.9(5)	1.919(4)	$7.25(10) \times 10^{-3}$	$9.10(10) \times 10^{-4}$	11.94
150	0.15	22.51(25)	2.019(29)	$-71.60(10) \times 10^{-3}$	$6.48(97) \times 10^{-3}$	14.37
150	0.10	13.90(18)	2.015(76)	$-113(22) \times 10^{-3}$	$10.5(1) \times 10^{-3}$	8.99
150	0.05	6.15(24)	2.278(33)	$-68.60(97) \times 10^{-3}$	$7.90(9) \times 10^{-3}$	3.92
150	0.035	5.10(42)	2.20(11)	$124(47) \times 10^{-1}$	$11.3(4) \times 10^{-1}$	7.98

## **CHAPTER 3: CONCLUSIONS**

As markets demand increases for better electronic performance, the continued use of  $\text{SiO}_2$  alone is unrealistic. The need for new, high-k dielectric materials is inevitable, and becoming a reality as development and experimentation of different materials continuous. Among these are attractive materials like  $\text{HfO}_2$  and  $\text{ZrO}_2$ , developed with the use of environmentally friendly techniques and attractive ambient depositions. It is clear that the development of inorganic precursors for the deposition of materials will be needed if this is to become an industry standard, whether the material is a binary metal oxide, a polymetal oxide, or even non-metals.

This work has demonstrated the development of inorganic aqueous precursors for the deposition of amorphous and crystalline thin-films via spin-coating. This method allows for thickness control by controlling precursor concentrations, as well as high-density films with aqueous solution deposition methods are promising candidates for electronic inclusion.

